Available online at www.sciencedirect.com
ScienceDirect
Tetrahedron
Tetrahedron 62 (2006) 10072–10078

Multi-state molecular switches based on dithienylperfluorocyclopentene and imidazo [4,5-*f*] [1,10] phenanthroline

Shuzhang Xiao, Tao Yi,* Yifeng Zhou, Qiang Zhao, Fuyou Li and Chunhui Huang*

Department of Chemistry and Laboratory of Advanced Materials, Fudan University, 220 Handan Road, Shanghai 200433, China

Received 6 June 2006; revised 16 August 2006; accepted 21 August 2006
Available online 7 September 2006

Abstract—Two novel diarylethene derivatives containing imidazo [4,5-*f*] [1,10] phenanthroline have been efficiently synthesized. These molecules are sensitive to both light and chemical stimuli. Under sequential alternating UV–vis light irradiation and alkali/acid treatment, distinct differences in NMR, UV–vis, and fluorescent spectra were observed. Taking advantage of the variations in visible absorption and fluorescence, a reversible four-state molecular switch with two optical outputs was realized by a single molecule.

1. Introduction

Molecular switches, which can be converted from one state to another by external stimuli such as light, electric field or chemical reaction, are becoming one of the most attractive fields in modern chemistry.[1–3] The use of photochromic compound as photon-mode switching system is considered to be a promising signaling mode for the molecular switches. In those systems, each isomer can represent either '*0*' or '*1*' of a digital binary code homologous to '*on*' and '*off*' states. Recently, the development of complex photochromic systems that integrate several switchable functions into a single molecule has attracted much attention because of the potential ability of such photochromic systems for applications in optical memory media and photonic devices.[4–7] Based on the reversible changes of the absorption and emission spectra of photochromic compounds under different external stimuli, the corresponding networks, including spiropyran,[8–17] diarylethene,[18] and some other complex systems[19–21] have been constructed. As a thermally irreversible system, diarylethenes may prove to be the most promising candidates for applications due to their good thermal stability and high fatigue resistance of both isomers. Irie et al. have reported that the digital switching of the fluorescence of diarylethene molecules can be controlled by irradiation with UV–vis light at the single-molecule level.[22] Tian et al. designed a single photochromic molecular switch with multi-optical outputs induced by light and chemical stimuli based on diarylethenes.[18,23] However, using only one photochromic diarylethene molecule to build a molecular switch with multi-optical outputs capable of building complex logic circuits is still a challenge. Moreover, the molecular switches, which can distinguish more than three kinds of states by digital output values, are rarely reported. In this report, we developed two novel photochromic diarylethene (**DAE**) molecules **1**·**2H** and **2**·**2H** containing imidazo [4,5-*f*] [1,10] phenanthroline (**IP**) moieties. In **1**·**2H**, **IP** and **DAE** moieties are directly linked to each other through a C–C σ bond without any intervening molecular bridge; whereas in the case of **2**·**2H**, a phenyl group connects the two moieties and mainly extends the conjugated system of **IP**. As we expected, both **1**·**2H** and **2**·**2H** were sensitive to both light irradiation and alkali simultaneously according to their structural characters, and gave multi-outputs of absorption and fluorescent emission signals (Scheme 1). Complex logic circuits were also built by using the single molecule based on the corresponding outputs.

2. Results and discussion

2.1. Synthesis of the diarylethene compounds

1·**2H** and **2**·**2H** were synthesized from 1,10-phenanthroline-5,6-dione and the corresponding aldehydes according to Scheme 2 in a good yield (70 and 80% for **1**·**2H** and **2**·**2H**, respectively). The molecular structures of these two compounds were confirmed by NMR spectroscopy and MALDI-TOF mass spectrometry, as well as by elemental analysis. Compared with **2**·**2H**, **1**·**2H** shows better solubility in methanol, ethanol, and DMSO.

Keywords: Molecular switches; Diarylethene; Fluorescence; Photochromism; Deprotonation.
* Corresponding authors. Tel.: +86 21 55664185; fax: +86 21 55664621; e-mail addresses: yitao@fudan.edu.cn; chhuang@fudan.edu.cn

0040–4020/$ - see front matter © 2006 Elsevier Ltd. All rights reserved.
doi:10.1016/j.tet.2006.08.061

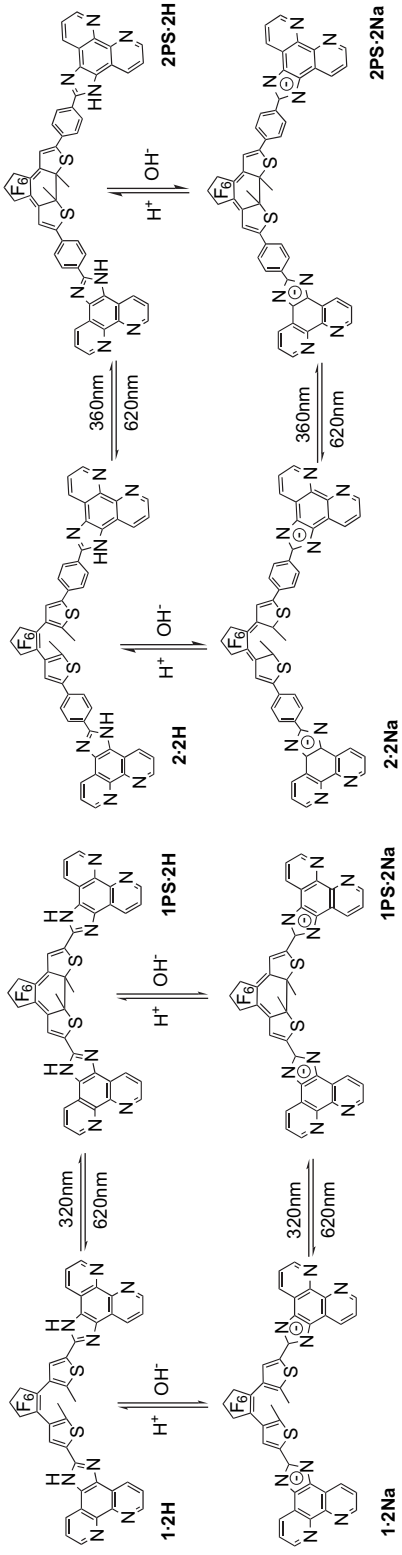

Scheme 1. The four states of **1** and **2** upon photochromism and deprotonation (**PS** is the abbreviation of photostationary state; **1**·**2Na**, **1PS**·**2Na**, and **2**·**2Na**, **2PS**·**2Na** are deprotonated isomers of **1**·**2H**, **1PS**·**2H**, and **2**·**2H**, **2PS**·**2H**, respectively).

2.2. NMR changes of 1·2H upon deprotonation by alkali

Deprotonation of the acidic imidazolyl N–H by addition of alkali changes the chemical shifts of the aryl protons of **1**·**2H**, which is revealed by the analysis of ^{1}H NMR spectra. Figure 1 displays the ^{1}H NMR spectral changes of **1**·**2H** in a DMSO-d_6 solution with titration of an NaOD solution. The ^{1}H NMR of **1**·**2H** exhibited an array of resonances corresponding to the aromatic protons in the molecule. The signal of NH in imidazolyl was not observed even prior to the addition of alkali. This may be due to fast proton exchange with water present in solution. Thienyl protons appear as a singlet at δ 8.04 (H1), and those for 2,8-positions of phenanthroline appear as multiplets centered at δ 7.80 (H3). A doublet at δ 8.80 with coupling constant of J=8.0 Hz is expected for H2 on phenanthroline. The other group of peaks at δ 9.03 should thus refer to H4 on phenanthroline. After adding NaOD into the DMSO-d_6 solution of **1**·**2H**, a clear upfield shift for H3 and H4 was observed. This is reasonable because the deprotonation enriches the electronic density of imidazolyl and leads to a higher shielding effect on these protons. The proton of H1 was incipiently upshifted and then shifted downfield while the amount of the base added was increased from 1 to 2 equiv. On the contrary, the signal for H2 was slowly shifted downfield. The different changes of the protons may be due to the anisotropic field effect of the anion to the π-system of phenanthroline. The resonances of the protons were constant after addition of more than 2 equiv of OH^-, which revealed a complete deprotonation of the imidazolyl. The altering chemical shift ($\Delta\delta$) of the protons for H1, H2, and H3 are -0.09, 0.08, and -0.08 ppm, respectively. The most significant change is that H4 on phenanthroline exhibited a significant upfield shift ($\Delta\delta$=-0.14 ppm), positing on the same signal position as H2. The NMR results indicate that the deprotonation promotes electron delocalization and averages the chemical environment of the protons on phenanthroline group of the molecule.[24]

2.3. Reversible absorption changes upon photochromism

The absorption spectra of both **1**·**2H** and **2**·**2H** show absorption bands only in the ultra violet range belonging to π–π^* transition (327 nm for **1**·**2H** and 343 nm for **2**·**2H**) (Fig. 2A and 2B). As expected, **1**·**2H** and **2**·**2H** showed reversible color and absorption spectral changes with the alternate irradiation of UV and visible lights (Scheme 1). Upon irradiation with light of 320 nm (360 nm for **2**·**2H**) within 5 min, the absorption at 598 nm (ε: 6100 dm^3 mol^{-1} cm^{-1}) and 612 nm (ε: 21,100 dm^3 mol^{-1} cm^{-1}) belonging to **1PS**·**2H** and **2PS**·**2H** (photostationary state), respectively, were observed accompanied with the deduction of the absorption bands in ultra violet range. Hence, the colorless solution of open-ring form became greenish blue due to the transformation of **1**·**2H** and **2**·**2H** by photocyclization into their closed-ring forms, with a quantum yields of 16 and 29%, respectively. The photocyclization conversion for **1**·**2H** and **2**·**2H** at photostationary state is 0.57 and 0.65, respectively. **1PS**·**2H** and **2PS**·**2H** were photochemically reverted to their open forms completely by 620 nm light irradiation with the quantum yields of 37 and 32%, respectively, and the greenish blue color disappeared. **2PS**·**2H** has a larger absorption efficiency and 14 nm red shift in visible range

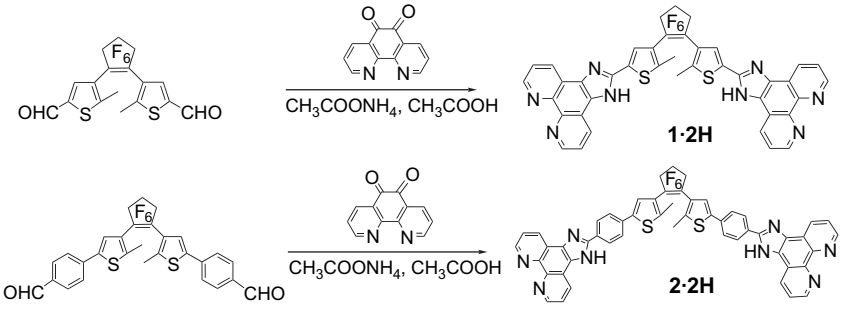

Scheme 2. Synthesis procedures of **1·2H** and **2·2H**.

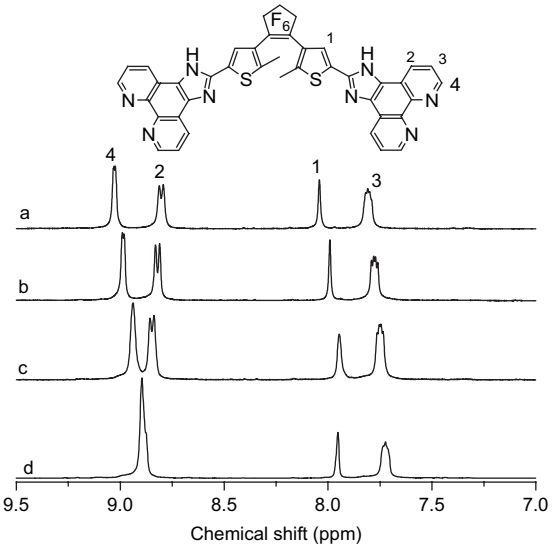

Figure 1. Partial ^{1}H NMR spectral changes of **1·2H** (2.5×10^{-2} mol/L) upon titration of NaOD (30%) at the equivalence of 0 (a), 0.6 (b), 1.0 (c), and 2.0 (d) of **1·2H** (400 MHz, DMSO-d_6 at 298 K).

compared with that of **1PS·2H**, showing a character of extended π-system. Both open and closed-ring forms of **1·2H**, **1PS·2H**, and **2·2H**, **2PS·2H** could be deprotonated to form **1·2Na**, **1PS·2Na**, and **2·2Na**, **2PS·2Na**, respectively, by adding alkali into their solutions. There is no appreciable difference in visible range of the absorption spectra between the corresponding protonated and deprotonated states in closed-ring forms of both molecules. This indicates that deprotonation has no notable effect on the ground state of closed **DAE** moiety in both molecules. The absorption band at UV region belonging to π–π* transition decreased a little in **1·2Na**, whereas this band decreases with an 8 nm red shift in **2·2Na**. The absorption spectra of **1·2H**, **1·2Na**, **2·2H**, **2·2Na**, and the corresponding photostationary states are shown in Figure 2C and 2D, respectively. The detailed quantitative data are given in Table 1.

2.4. Reversible fluorescent changes during photochromism and deprotonation

Generally, the open isomer of diarylethene emits fluorescence, while the fluorescence of closed-ring form is inactive. In the present work, **1·2H** and **2·2H** exhibited fluorescent changes during the process of photoisomerization as most of the diarylethene derivatives did.[25–40] The fluorescent emissions of **1·2H** and **2·2H** were at 516 and 510 nm with fluorescent quantum yields of 0.038 and 0.014, respectively (Table 2). The fluorescent lifetimes of **1·2H** and **2·2H** at 510 nm are 0.58 and 3.52 ns, respectively. To further understand the ascription of these emissions in **1·2H** and **2·2H**, the fluorescent properties of two model compounds of 2-methylthienyl-5-**IP** and *p*-bromophenyl-**IP** were investigated. These two compounds have fluorescent emissions at 436 and 438 nm, respectively. Comparing with the model compounds, the emission bands in **1·2H** and **2·2H** are red shifted about 70 nm, which indicates that the effect of the coupling of the **IP** substituent to the central **DAE** unit is much pronounced in fluorescence.[39] From careful comparison of the spectral shape of **1·2H** and **2·2H**, we observed much larger $W_{1/2}$ (peak width at half height) in the spectrum of **1·2H** (193 nm) than that of **2·2H** (106 nm), which reveals that the emission of **1·2H** may come from two sources. The inconspicuous shoulder peak at about 460 nm in **1·2H** accords with the characteristic local fluorescent emission of **IP**.[41,42] As expected, both the fluorescent emissions of **1·2H** and **2·2H** are quenched by photocyclization. The intensity of the emission in **2·2H** was quenched to ca. 7% of the original state upon irradiation with 360 nm UV light (Fig. 3A). However, the fluorescent intensity only decreased ca. 54% at its PS state in **1·2H** (Fig. 3B). The comparatively low photocyclization conversion and the existence of parallel configuration of **DAE** in **1·2H** may be the main cause for the unnotable fluorescent change induced by photo irradiation in **1·2H**. **2·2H** shows more significant fluorescent switch upon photochromism than that of **1·2H** because of the larger absorption efficiency and higher photocyclization conversion.

The deprotonation of imidazole in **1·2H** and **2·2H** also made significant emissive difference. The emission at 510 nm in **2·2H** decreased greatly with addition of alkali. The fluorescent Φ_F of **2·2Na** reduces to only 5% of that of **2·2H** (Fig. 4A). This efficient fluorescent quench is a result of photo induced electron transfer (PET) process[43] from deprotonated imidazole to **DAE** group because the deprotonation of imidazolyl group enhanced the electron density in **IP** group. It is interesting that the deprotonation process in **1·2H** resulted in a more complicate fluorescent change. The emission at 516 nm in **1·2H** decreased greatly with addition of alkali, and the shoulder peak at 460 nm emerged with fluorescent quantum yield of 0.025 in **1·2Na** (Fig. 4B). The emission spectra were no longer changed after more than 2 equiv of alkali were added in both **1·2H** and **2·2H**, consistent with ^{1}H NMR titration spectra. The lifetimes of both **1·2Na** and **2·2Na** at 510 nm are a little extended

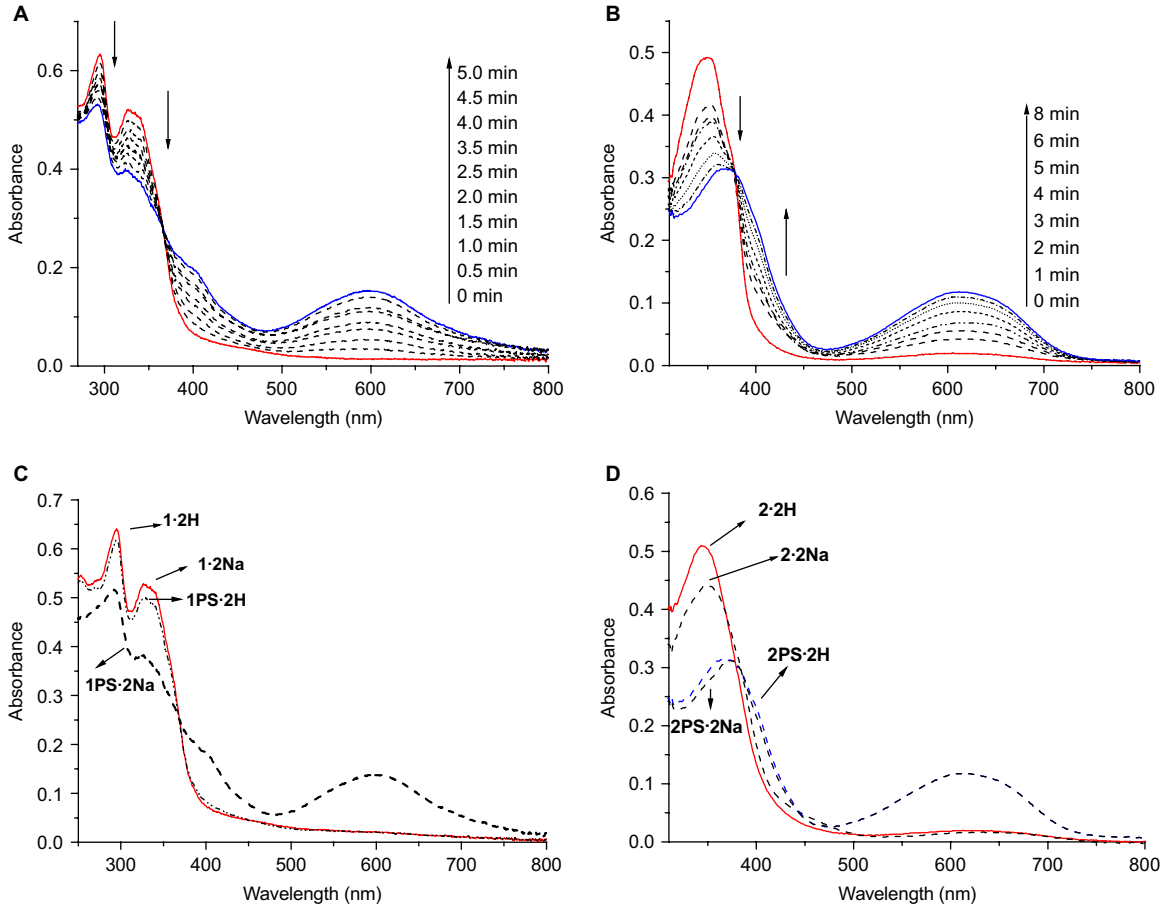

Figure 2. Absorption spectral changes upon irradiation of 320 nm for **1·2H** (A) and 360 nm for **2·2H** (B). Absorption spectra of **1** (C) and **2** (D) at the four states corresponding to Scheme 1. ([**1**]: 4.0×10^{-5} mol/L in methanol, [**2**]: 1.0×10^{-5} mol/L in methanol, 298 K, 2 equiv of the base was added for the corresponding deprotonated states).

Table 1. The quantitative data upon photochromism in **1** and **2**

Compound	λ_{max}^{abs}	ε (dm^3 mol^{-1} cm^{-1})	$\Phi_{o\rightarrow c}$ or $\Phi_{c\rightarrow o}$ [a]	Conversion (o→c) [b]
1·2H	327	14,000	0.16 (o→c)	0.57
1PS·2H	598	6100	0.29 (c→o)	1.00
1·2Na	327	13,400		
1PS·2Na	599	6100		
2·2H	343	68,000	0.29 (o→c)	0.65
2PS·2H	612	21,100	0.34 (c→o)	1.00
2·2Na	349	58,700		
2PS·2Na	612	21,100		

[a] Calculated from absorption spectral change.
[b] Obtained from the result of ^{1}H NMR.

Table 2. Fluorescent properties of **1** and **2**

Compound	λ_{max}^{F}	Φ_F [a]	τ (ns) (510 nm, λ_{ex}=370 nm)
1·2H	516	0.038	0.58
1·2Na	460	0.025	1.11
2·2H	510	0.014	3.52
2·2Na	550	<0.001	3.78

[a] $\Phi_F=\Phi_{ref}[(n^2A_{ref}I/n_{ref}^2AI_{ref})]$ (n, A, I denote the refractive index of solvent, the absorbance at the excitation wavelength, and the area of the corrected emission spectrum, respectively. Disulfate quinine was used as a reference (ref), Φ_{ref}=0.577).

comparing with that of **1·2H** and **2·2H** (Table 2). The behaviors of deprotonation-induced fluorescent spectral changes in **1PS·2H** and **2PS·2H** are similar to those of **1·2H** and **2·2H**, respectively.

The remarkably reversible emission quenching process by both photocyclization and deprotonation (Fig. 5A) makes **2·2H** a potential candidate for binary logic process as well as fluorescent switch and specific sensor on alkali. Moreover, both intensity and emission wavelengths of **1·2H** could be reversibly regulated by UV and visible lights, alkali and proton, respectively (Fig. 5B). This multi-output character of **1·2H** also makes it a possible candidate for binary logic process.

2.5. Multi-state molecular switches and logic circuit

The absorption and fluorescent changes of **2·2H** can be combined as a complicated molecular switch induced by three inputs: *I*1 (340 nm UV light), *I*2 (620 nm visible light), and *I*3 (alkali). Responding to these inputs, two corresponding optical outputs *O*1 (absorption difference ΔA at 610 nm by UV light irradiation) and *O*2 (emission variation ΔF_{510} at 510 nm) are produced. *O*1 is *on* in the case of $\Delta A>0.06$ (50% of that in photostationary state). When fluorescent intensity at 510 nm is quenched to half of the original height (**2·2H**), i.e. $\Delta F_{510}<0.5$, *O*2 is *off*, whereas *O*2 is *on* when

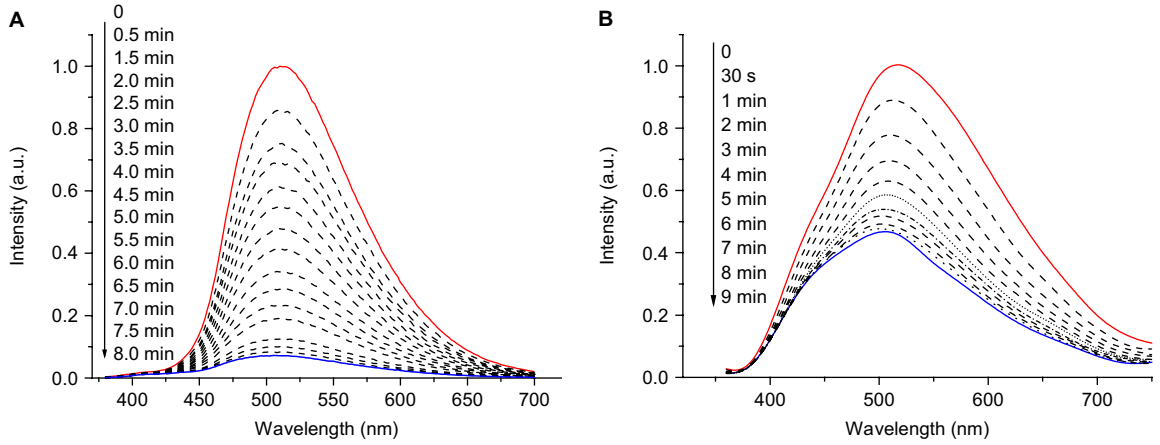

Figure 3. Fluorescent spectral changes of **2·2H** (A) and **1·2H** (B) upon irradiation of 360 and 320 nm light, respectively. ([**1**]: 4.0×10^{-5} mol/L in methanol, Ex: 320 nm; [**2**]: 1.0×10^{-5} mol/L in methanol, Ex: 360 nm, the fluorescent intensites of **1·2H** at 516 nm and **2·2H** at 510 nm were integrated to 1.0, for clear comparison. All the experiments are performed at room temperature.)

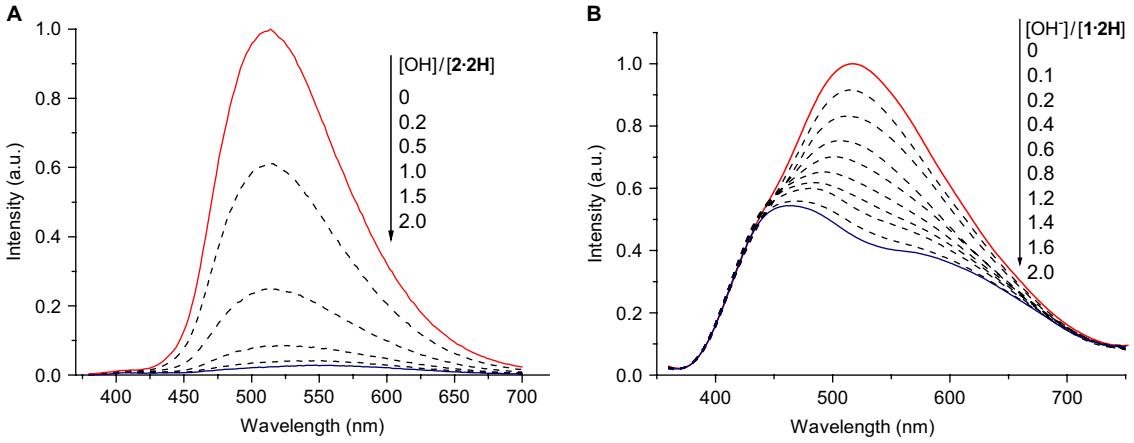

Figure 4. The emissive spectral changes during the deprotonation process of **2·2H** (A) and **1·2H** (B) upon titration of alkali equivalent to the corresponding molecule from 0 to 2.0 equiv (in the same condition as for Fig. 3).

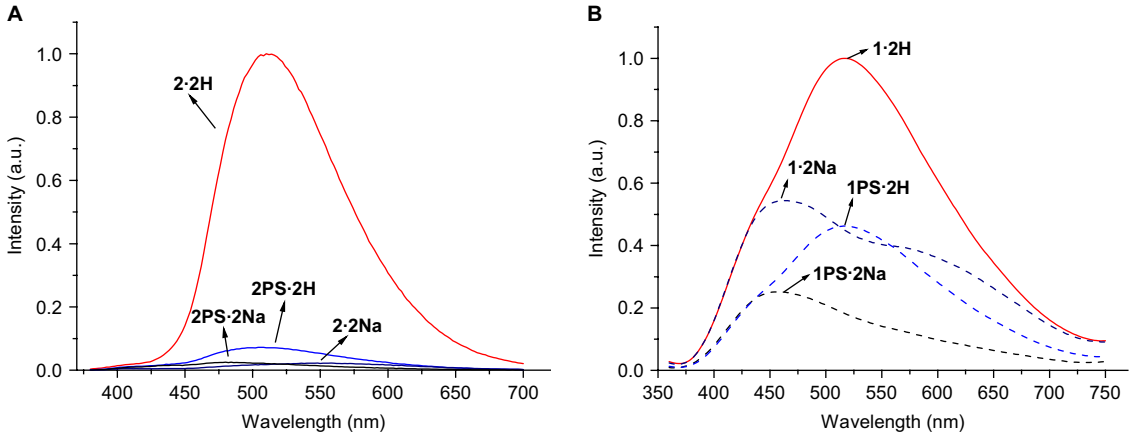

Figure 5. The fluorescent spectra of **1·2H** (A) and **2·2H** (B) at their four states corresponding to Scheme 1; for the conditions see Figure 3.

$\Delta F_{510}>0.5$. Each signal can be represented by a binary digit as either *on* or *off*. Therefore, the molecular switch reads a string of three binary inputs and writes a specific combination of two binary outputs (Table 3). Within that binary data, it is clear that the coloration ($O1=1$) and bleaching ($O1=0$) switch is dependent only on alternating UV–vis irradiation, while $I3$ gives no influence on $O1$. The low value of $I2$ (*off*) and high value of $I1$ (*on*) always tend to a high value of $O1$ (*on*). Upon simultaneous irradiation with UV and visible lights, absorption at 610 nm is in low value, indicating that

Table 3. Truth table for the communicating molecular switch in **2**

Inputs			Outputs	
*I*1	*I*2	*I*3	*O*1 (ΔA_{610})	*O*2 (ΔF_{510})
0	*0*	*0*	*0* (Low, <0.06)	*1* (High, >0.5)
0	*0*	*1*	*0*	*0* (Low, <0.5)
0	*1*	*0*	*0*	*1*
1	*0*	*0*	*1* (High, >0.06)	*0*
0	*1*	*1*	*0*	*0*
1	*0*	*1*	*1*	*0*
1	*1*	*0*	*0*	*1*
1	*1*	*1*	*0*	*0*

*I*1, *I*2, and *I*3 are the 340 nm UV light, 620 nm visible light, and alkali, respectively; *O*1, *O*2 are referred to the absorption and fluorescent difference at 610 and 510 nm, respectively.

*O*1 is *off* in this case. Thus the output *O*1 distinguishes the two kinds of states in the molecular switch, **2·2H** or **2·2Na**, *O*1=*0* and **2PS·2H** or **2PS·2Na**, *O*1=*1*. Therefore the input data *I*1, *I*2 are transduced into the output data *O*1 through an INHIBIT logic circuit by NOT and AND operators.[4] The other output *O*2 (ΔF_{510}) is varied along with *I*2 and *I*3 because the fluorescent intensity at 510 nm is quenched by both UV light and addition of alkali. Thus, *O*2 can be produced through a NOR operator by *I*1 or *I*3. Combining the output *O*1 and *O*2, the four states **2·2H**, **2PS·2H**, **2·2Na**, and **2PS·2Na** are addressed by three output strings *01*, *00*, and *10*, respectively, in the molecular switch.

3. Conclusion

In conclusion, we have obtained two multi-state diarylethenes (**1·2H** and **2·2H**) responsive to both light and chemical input, by utilizing the obviously different absorption and fluorescent emission under sequential alternating UV–vis irradiation and alkali/proton. The effective fluorescent quenching process upon both photochromism and deprotonation in **2·2H** provides a potential application in fluorescent switch or alkali sensor. Additionally, a reversible four-state molecular switch with two optical outputs is also realized in **2·2H**. This molecular level signal communication in the molecular switches is important for information storage and practical devices, even though the present systems still exihibit several limits such as working in solution media and long equilibrium time of deprotonation. The modification of the analogous molecules into soft materials such as gel or micro (nano) system may fulfill their practical application, especially in biological system. Moreover, phenanthroline group of these diarylethenes could coordinate with various metal ions to form metal complexes. These complexes would show more exciting characteristics on energy transfer and molecular switches. Further work is currently in progress toward the assembled soft materials and the coordinated systems of these diarylethenes.

4. Experimental

4.1. General

All starting materials were obtained from commercial supplies and used as received. Column chromatography was carried out on silica gel (200–300 mesh). ^{1}H NMR and ^{13}C NMR spectra were recorded on a Mercuryplus-Varian instrument (400 MHz). Proton chemical shifts are reported in parts per million downfield from tetramethylsilane (TMS). MALDI-TOF-MS was recorded on AXIMA-CFRPLVS mass spectroscopy instrument (Shimadzu). UV–vis spectra were recorded on UV–Vis 2550 spectroscope (Shimadzu). Fluorescent spectra were measured on Edinburgh Instruments (FLS 900). Time-resolved fluorescent decay was recorded on Edinburgh LifeSpec-ps with a PDL 800-B pulsed diode laser as excitation source. The UV and visible irradiations were carried out on a CHF-XM550W power system (China) by using suitable band-pass filter (Omega).

4.2. Synthesis

The aldehyde derivatives were synthesized according to references.[44,45] *1,2-Bis(5′-formyl-2′-methylthien-3′-yl)perfluorocyclopentene*: ^{1}H NMR ($CDCl_3$, 400 MHz, 298 K): δ 2.02 (s, 6H), 7.73 (s, 2H), 9.85 (s, 2H). *1,2-Bis[5′-(4-formylphenyl)-2′-methylthien-3′-yl]perfluorocyclopentene*: ^{1}H NMR ($CDCl_3$, 400 MHz, 298 K): δ 2.00 (s, 6H), 7.43 (s, 2H), 7.68–7.70 (d, J=8 Hz, 4H), 7.88–7.90 (d, J=8 Hz, 4H), 10.00 (s, 2H). *1,10-Phenanthroline-5,6-dione* was obtained according to previous report.[46] Mp 254–256. ^{1}H NMR (400 MHz, $CDCl_3$, 298 K): δ 7.57–7.60 (q, $J1$=8.0 Hz, $J2$=4.8 Hz, 2H), 8.49–8.51 (d, J=8.0 Hz, 2H), 9.11–9.12 (d, J=4.8 Hz, 2H).

4.2.1. 1,2-Bis(5-(1*H*-imidazo [4,5-*f*] [1,10] phenanthroline-2-yl)-2-methylthien-3-yl)perfluorocyclopentene (1·2H). Acetic acid (15 mL) was added to a mixture of the aldehyde derivative (0.32 g, 0.75 mmol), 1,10-phenanthroline-5,6-dione (0.29 g, 1.4 mmol), and ammonium acetate (2.0 g, 26 mmol). The reaction mixture was stirred at reflux (80–90 °C) for 3 h. Then ice water was poured in, and a pale yellow solid of raw product was obtained by filtration. **1·2H** was recrystallized from ethanol as a pale yellow solid (yield: 70%). Mp>280 °C. ^{1}H NMR (400 MHz, CD_3SOCD_3, 298 K): δ 1.89 (s, 6H), 7.80–7.82 (q, $J1$=8.0 Hz, $J2$=3.2 Hz, 4H), 8.04 (s, 2H), 8.80–8.82 (d, J=8.0 Hz, 4H), 9.03–9.04 (d, J=3.2 Hz, 4H). ^{13}C NMR (100 MHz, CD_3SOCD_3): δ 14.98, 116.60, 123.84, 125.28, 125.39, 130.19, 130.43, 133.06, 143.26, 144.13, 144.63, 145.52, 148.43, 148.56, 172.87. MALDI-TOF: m/z=805.1 $[M]^+$. Anal. Calcd for $C_{41}H_{22}F_6N_8S_2\cdot 4AcOH\cdot 2H_2O$: C, 54.54; H, 3.74; N, 10.38. Found: C, 54.96; H, 3.77; N, 9.91.

4.2.2. 1,2-Bis(5-(4-(1*H*-imidazo [4,5-*f*] [1,10] phenanthroline-2-yl) phenyl)-2-methylthien-3-yl)perfluorocyclopentene (2·2H). Raw product of **2·2H** was obtained by the same method as that of **1·2H**, and was purified by recrystallization from DMF–H_2O to give a pale yellow solid (yield: 80%). Mp>280 °C. ^{1}H NMR (400 MHz, CD_3SOCD_3, 298 K): δ 1.89 (s, 6H), 7.69 (s, 2H), 7.79–7.82 (m, 4H), 7.87–7.89 (d, J=8.4 Hz, 4H), 8.31–8.33 (d, J=8.0 Hz, 4H), 8.91–8.93 (d, J=8.0 Hz, 4H), 9.01–9.02 (t, 4H). ^{13}C NMR (100 MHz, CD_3SOCD_3): δ 14.68, 122.00, 123.56, 125.79, 126.02, 127.37, 127.41, 128.01, 129.94, 130.26, 132.17, 133.68, 136.82, 141.81, 142.31, 144.02, 148.08, 150.40, 173.28. MALDI-TOF mass: m/z=957.2 $[M]^+$. Anal. Calcd for $C_{53}H_{30}F_6N_8S_2\cdot DMF\cdot 3H_2O$: C, 62.04; H, 4.00; N, 11.63. Found: C, 61.92; H, 4.08; N, 11.08.

Acknowledgements

This work was financially supported by the National Science Foundation of China (20571016, 20441006, and 20490210), SRF for ROCS, SEM, and Shanghai Sci. Tech. Comm. (05DJ14004).

References and notes

1. Feringa, B. L. *Molecular Switches*; Wiley-VCH: Weinheim, 2001.
2. Irie, M. *Chem. Rev.* **2000**, *100*, 1685–1716.
3. Tian, H.; Yang, S. J. *Chem. Soc. Rev.* **2004**, *33*, 85–97.
4. Raymo, F. M. *Adv. Mater.* **2002**, *14*, 401–414.
5. de Silva, A. P.; Mcclenaghan, N. D. *Chem.—Eur. J.* **2004**, *10*, 574–586.
6. Szacilowski, K. *Chem.—Eur. J.* **2004**, *10*, 2520–2528.
7. Xiao, S.; Yi, T.; Li, F.; Huang, C. *Tetrahedron Lett.* **2005**, *46*, 9009–9012.
8. Raymo, F. M.; Giorgani, S. *J. Am. Chem. Soc.* **2001**, *123*, 4651–4652.
9. Raymo, F. M.; Giorgani, S. *Org. Lett.* **2001**, *3*, 1833–1836.
10. Raymo, F. M.; Giorgani, S. *Org. Lett.* **2001**, *3*, 3475–3478.
11. Raymo, F. M.; Giorgani, S. *J. Org. Chem.* **2003**, *68*, 4158–4169.
12. Raymo, F. M.; Giorgani, S. *J. Am. Chem. Soc.* **2002**, *124*, 2004–2007.
13. Guo, X.; Zhang, D.; Wang, T.; Zhu, D. *Chem. Commun.* **2003**, 914–915.
14. Guo, X.; Zhang, D.; Zhou, Y.; Zhu, D. *J. Org. Chem.* **2003**, *68*, 5681–5687.
15. Guo, X.; Zhang, D.; Zhang, G.; Zhu, D. *J. Phys. Chem. B* **2004**, *108*, 11942–11945.
16. Guo, X.; Zhang, D.; Zhu, D. *Adv. Mater.* **2004**, *16*, 125–129.
17. Zhou, Y.; Zhang, D.; Zhang, Y.; Tang, Y.; Zhu, D. *J. Org. Chem.* **2005**, *70*, 6164–6170.
18. Tian, H.; Qin, B.; Yao, R.; Zhao, X.; Yang, S. *Adv. Mater.* **2003**, *15*, 2104–2107.
19. Pina, F.; Roque, A.; Melo, M. J.; Maestri, M.; Belladelli, L.; Balzani, V. *Chem.—Eur. J.* **1998**, *4*, 1184–1191.
20. Cheng, P. N.; Chiang, P. T.; Chiu, S. H. *Chem. Commun.* **2005**, 1285–1287.
21. Qu, D. H.; Wang, Q. C.; Tian, H. *Angew. Chem., Int. Ed.* **2005**, *44*, 5296–5299.
22. Irie, M.; Fukaminato, T.; Sasaki, T.; Tamai, N.; Kawai, T. *Nature* **2002**, *420*, 759–760.
23. Luo, Q. F.; Li, X. C.; Jing, S. P.; Zhu, W. H.; Tian, H. *Chem. Lett.* **2003**, *32*, 1116–1117.
24. Liu, F.; Wang, K.; Bai, G.; Zhang, Y.; Gao, L. *Inorg. Chem.* **2004**, *43*, 1799–1806.
25. FernaÂndez-Acebes, A.; Lehn, J. M. *Chem.—Eur. J.* **1999**, *5*, 3285–3292.
26. FernaÂndez-Acebes, A.; Lehn, J. M. *Adv. Mater.* **1998**, *10*, 1519–1522.
27. Murguly, E.; Norsten, T. B.; Branda, N. R. *Angew. Chem., Int. Ed.* **2001**, *40*, 1752–1755.
28. Norsten, T. B.; Branda, N. R. *Adv. Mater.* **2001**, *13*, 347–349.
29. Chen, B.; Wang, M.; Wu, Y.; Tian, H. *Chem. Commun.* **2002**, 1060–1061.
30. Uchida, K.; Saito, M.; Murakami, A.; Nakamura, S.; Irie, M. *Adv. Mater.* **2003**, *15*, 121–125.
31. Chen, S. H.; Chen, H. M. P.; Geng, Y.; Jacobs, S. D.; Marshall, K. L.; Blanton, T. N. *Adv. Mater.* **2003**, *15*, 1061–1065.
32. Uchida, K.; Saito, M.; Murakami, A.; Kobayashi, T.; Nakamura, S.; Irie, M. *Chem.—Eur. J.* **2005**, *11*, 534–542.
33. Wigglesworth, T. J.; Branda, N. R. *Adv. Mater.* **2004**, *16*, 123–125.
34. Tian, H.; Chen, B.; Tu, H.; Mullen, K. *Adv. Mater.* **2002**, *14*, 918–923.
35. Lim, S. J.; An, B. K.; Jung, S. D.; Chung, M. A.; Park, S. Y. *Angew. Chem., Int. Ed.* **2004**, *43*, 6346–6350.
36. Fukaminato, T.; Sasaki, T.; Kawai, T.; Tamai, N.; Irie, M. *J. Am. Chem. Soc.* **2004**, *126*, 14843–14849.
37. Frigoli, M.; Hehi, G. H. *Chem.—Eur. J.* **2004**, *10*, 5243–5250.
38. Yagi, K.; Soong, C. F.; Irie, M. *J. Org. Chem.* **2001**, *66*, 5419–5423.
39. Ern, J.; Bens, A. T.; Martin, H. D.; Mukamel, S.; Tretiak, S.; Tsyganenko, K.; Kuldova, K.; Trommsdorff, H. P.; Kryschi, C. *J. Phys. Chem. A* **2001**, *105*, 1741–1749.
40. Giordano, L.; Jovin, T. M.; Irie, M.; Jares-Erijman, A. E. *J. Am. Chem. Soc.* **2002**, *124*, 7481–7489.
41. Liu, Y.; Duan, Z. Y.; Zhang, H. Y.; Jiang, X. L.; Han, J. R. *J. Org. Chem.* **2005**, *70*, 1450–1455.
42. Mondal, J. A.; Ramakrishna, G.; Singh, A. K.; Ghosh, H. N.; Mariappan, M.; Maiya, B. G.; Mukherjee, T.; Palit, D. K. *J. Phys. Chem. A* **2004**, *108*, 7843–7852.
43. de Silva, A. P.; Gunaratne, H. Q. N.; Gunnlaugsson, T.; Huxley, A. J. M.; McCoy, C. P.; Rademacher, J. T.; Rice, T. E. *Chem. Rev.* **1997**, *97*, 1515–1566.
44. Gilat, S. L.; Kawai, S. H.; Lehn, J. M. *Chem.—Eur. J.* **1995**, *1*, 275–284.
45. Yamamoto, S.; Matsuda, K.; Irie, M. *Chem.—Eur. J.* **2003**, *9*, 4878–4886.
46. Hiort, C.; Lincoln, P.; Norden, B. *J. Am. Chem. Soc.* **1993**, *115*, 3448–3454.